Biointerface Research in Applied Chemistry
Open-Access Journal (ISSN: 2069-5837)

*Article*
**Volume 14, Issue 5, 2024, 124**
https://doi.org/10.33263/BRIAC145.124

# Stability of Structure, Chemical Properties, and Biological Effects of Diacyl Derivatives of Dibenzo-18-crown-6

**Nafisa R. Komilova [1,2], Lyubov K. Kozinskaya [3], Aynisa K. Tashmuhamedova [3], Andrey Y. Abramov [4], Ulugbek Z. Mirkhodjaev [1]**

1 Department of Biophysics, National University of Uzbekistan, Tashkent, Uzbekistan
2 Center for Advanced Technologies, Tashkent, Uzbekistan
3 Department of general and oil-gas chemistry, National University of Uzbekistan, Tashkent, Uzbekistan
4 Department of Clinical and Movement Neurosciences, UCL Queen Square Institute of Neurology, London, UK
* Correspondence: na.komilova@nuu.uz;

Scopus Author ID 57270150500
**Received: 4.11.2023; Accepted: 28.01.2024; Published: 22.07.2024**

**Abstract:** The interplay between $Ca^{2+}$ ions and neuronal dysfunction has recently gained significant attention. A growing body of evidence implicates $Ca^{2+}$ in the pathophysiology of neurodegenerative disorders, including Parkinson's disease. The rate of protein aggregate formation, mitophagy, and autophagy abnormalities in Parkinson's disease may be influenced by $Ca^{2+}$ ions, and specific ionophores have been used to study this phenomenon. We investigated the potential of diacyl derivatives of dibenzo-18-crown-6 (DB18C6), namely 4′,4″(5″)-dibutyryl-DB18C6 and 4′,4″(5″)-divaleryl-DB18C6 and 4′,4″-diacetyl-DB18C6 as an alternative to these specific ionophores. Our study provides evidence that both 4′,4″(5″)-dibutyryl-DB18C6 and 4′,4″(5″)-divaleryl-DB18C6 can effectively promote $Ca^{2+}$ transport across fibroblast cell membranes at 10 and 100 nanomolar concentrations. Notably, the studied crown ethers do not appear to impact intracellular pH or mitochondrial membrane potential. Also, we assessed these molecules' structural stability and chemical purity, confirming their integrity and suitability for future research. These results suggest that using crown ethers as ionophores may be a promising alternative to specific ionophores in studying the impact of $Ca^{2+}$ ions on various cellular processes in Parkinson's disease.

**Keywords:** crown ethers; ionophores; calcium; 4',4"-diacetyl-DB18C6; 4', 4"(5")-dibutyryl-DB18C6; 4',4"(5")-divaleryl-DB18C6; NMR spectra.



## 1. Introduction

Mitochondrial dysfunction and oxidative stress are known to contribute to the loss of dopaminergic neurons in the substantia nigra pars compacta, leading to the characteristic motor symptoms of the disease. Although dopamine is often considered the central player in this process, accumulating evidence suggests that $Ca^{2+}$ is a critical mediator of neuronal degeneration. For example, α-synuclein, a cytosolic protein with 140 amino acid residues implicated in the pathophysiology of Parkinson's disease, has been shown to create α-helical channels in the plasma membrane, allowing extracellular $Ca^{2+}$ transfer and, therefore, increase cytosolic $Ca^{2+}$ concentration [1]. A recent study has also discovered the existence of α-synuclein in mitochondria and the mitochondrial ER membrane [2,3]. Paillusson *et al*. found that α-synuclein-induced loosening of ER-mitochondria connections disrupts $Ca^{2+}$ exchange

between these two organelles, affecting the PD phenotype significantly [4]. PD has also been demonstrated to have higher cytosolic $Ca^{2+}$ influx due to increased L-type $Ca^{2+}$ channel activity [5]. Increased cytosolic $Ca^{2+}$ content, on the other hand, has an effect on cell bioenergetics by increasing ATP demand [6].

Furthermore, the change in cytosolic $Ca^{2+}$ impairs normal $Ca^{2+}$ handling by many intracellular organelles, endangering neuronal survival [7-10]. There is a lot of evidence suggesting mitochondria's functional role in PD, especially mitochondrial oxidative stress. Inhibiting mitochondrial $Ca^{2+}$ intake reduces oxidative stress in Substantia nigra pars compacta, suggesting that mitochondrial oxidative stress may be caused by mitochondrial $Ca^{2+}$ excess rather than the necessity for increased ATP generation alone [11,12].

Despite this, many gaps remain in our understanding of the involvement of $Ca^{2+}$ in Parkinson's disease. Addressing these knowledge gaps may facilitate the development of novel therapies to prevent or mitigate the onset of the disease and promote successful aging more broadly. In this context, alternative ionophores, including crown ethers, have been investigated for their potential to affect intracellular $Ca^{2+}$ levels. This study aims to evaluate the ability of specific crown ethers to act as ionophores for $Ca^{2+}$ ions and to discuss the implications of these compounds for understanding the role of $Ca^{2+}$ in neurodegenerative disorders and some types of cancer [13,14].

## 2. Materials and Methods

### *2.1. Cell culture.*

Fibroblasts were obtained from a 4 mm skin punch biopsy performed under local anesthesia, following ethical approval from the local committee. Informed consent was obtained from all participating patients. The study received ethical clearance for patient investigations and skin sample collection for research purposes from the University College London Hospital ethics committee (Approval Number: 07/N018). Biopsy samples were cut into approximately 1 mm pieces and cultured in DMEM supplemented with 10% FBS and 1% GlutaMAX until fibroblasts began to grow from the explants. Upon reaching confluency, fibroblasts were harvested from the culture dishes using TrypLE Express (Invitrogen) and then transferred to larger culture vessels for further propagation and cryopreservation.

### *2.2. Measurement of intracellular $Ca^{2+}$ and mitochondrial membrane potential.*

Fibroblasts were loaded with Fura – 2 AM (5µg/ml) and pluronic acid (2,5 µg/ml) in a HEPES-buffered salt solution (HBSS) for 15 min. Before starting the experiment, cells were treated with rhodamine123 (Rh123; 1 µg/ml; Molecular Probes) for 15 min. After loading, cells were washed five times before the experiment. Under these loading conditions, Fura – 2 AM and Rh123 are nontoxic and provide reliable and reproducible measures of mitochondrial calcium through dequenching mitochondrial fluorescence. Rh123 was used in the dequenching mode to measure $\Delta\Psi m$; thus, an increase in the Rh123 signal reflects mitochondrial depolarization. Three types of crown ethers 4',4"-diacetyl-DB18C6; 4',4"(5")-dibutyryl-DB18C6 and 4',4"(5")-divaleryl-DB18C6 were investigated as ionophores for $Ca^{+2}$ ions.

*2.3. Measurement of intracellular pH.*

Cells were loaded for 30 min at room temperature with 5 μM 5-(and-6-)-carboxyl SNARF-1 AM and 0.005% pluronic acid in a Hank's Balanced Salt Solution (HBSS) composed of (mM): 156 NaCl, 3 KCl, 1 $MgSO_4$, 1.25 $KH_2PO_4$, 2 $CaCl_2$, 10 glucose, and 10 HEPES; pH adjusted to 7.4 with NaOH. $NH_4Cl$ was added and washed out to calibrate the SNARF ratio.

Fluorescence measurements were obtained on an epifluorescence inverted microscope equipped with a ×20 fluorite objective. $[Ca^{2+}]_i$ and Δψm were monitored in single cells using excitation light provided by a Xenon arc lamp, the beam passing sequentially through 10 nm bandpass filters centered at 340, 380, and 490 nm housed in computer-controlled filter wheels (Cairn Research, Kent, UK). Emitted fluorescence light was reflected through a 515 nm long-pass filter to a cooled CCD camera (Retiga, QImaging, Canada). Fluorescence was collected every 10 s in the experiment. All imaging data were collected and analyzed using software from Andor (Belfast, UK). The fura-2 data have not been calibrated in terms of $[Ca^{2+}]$ cyt because of the uncertainty arising from the use of different calibration techniques. We have normalized the signals between the resting level (set to 0) and a maximal signal (which corresponds to full mitochondrial depolarization) generated in response to the protonophore FCCP (1 μM; set to 100%).

*2.4. Statistical analysis.*

Statistical analysis and exponential curve fitting were performed using Origin 8 (Microcal Software Inc., Northampton, MA) software. Data was generated from a minimum of three independent replicates per experiment ($n \geq 3$) performed on different days. Each replicate consisted of at least one coverslip per condition where 15–30 cells were analyzed. For all graphs, error bars represent mean ±SEM.

*2.5. Ethical approval and informed consent.*

The Biobank of cells from the National Hospital for Neurology and Neurosurgery and the Institute of Neurology kindly provided primary fibroblast lines, UCL, London, UK.

*2.6. Identification of the structure of DB18C6 diacyl derivatives.*

IR spectra were analyzed to investigate crown ethers $^1H$- and $^{13}C$- NMR spectra. SDS and deuterated water ($D_2O$, degree of substitution 99.9%) were purchased from Sigma-Aldrich. All NMR samples were prepared in 5-mm NMR tubes.

## 3. Results and Discussion

*3.1. The effect of diacyl derivatives of DB18C6 on $Ca^{2+}$ ion transport across the membrane of fibroblasts.*

Experiments were carried out on a healthy fibroblast cell, and as a result, it has been found that both crown ethers, in a dose-dependent manner, increase the cytoplasmic concentration of $Ca^{2+}$ by increasing $Ca^{2+}$ transport across the membrane (Figure 1).

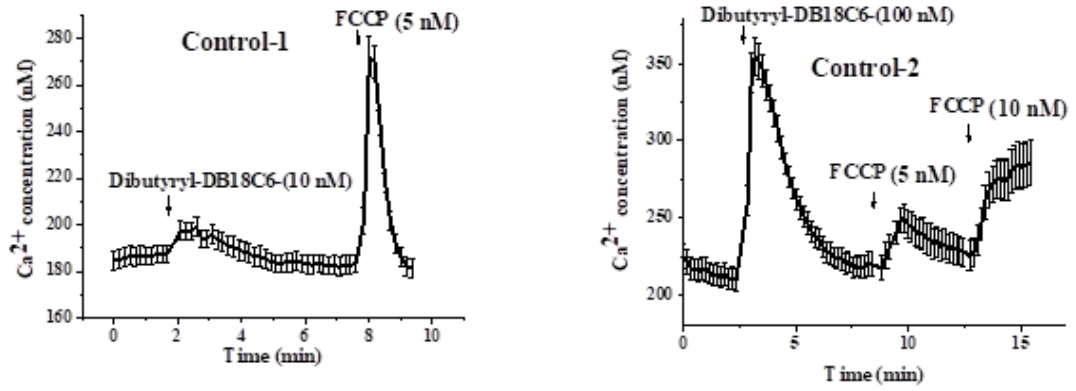


**(a)** **(b)**

**Figure 1. (a)** The effect of 4′,4″(5″)-dibutyryl-DB18C6 on the $[Ca^{2+}]_{cyt}$ in healthy fibroblasts at 10 nM; **(b)** 100 nM concentrations. n=60.

Fura-2 AM and Rhodamine 123 are widely used fluorescent indicators that enable reproducible measurements of mitochondrial calcium and mitochondrial membrane potential, respectively. Changes in the fluorescence intensity of Rhodamine 123 directly correlate with alterations in mitochondrial membrane potential, providing a reliable measure of mitochondrial health and functionality (Figure 2).

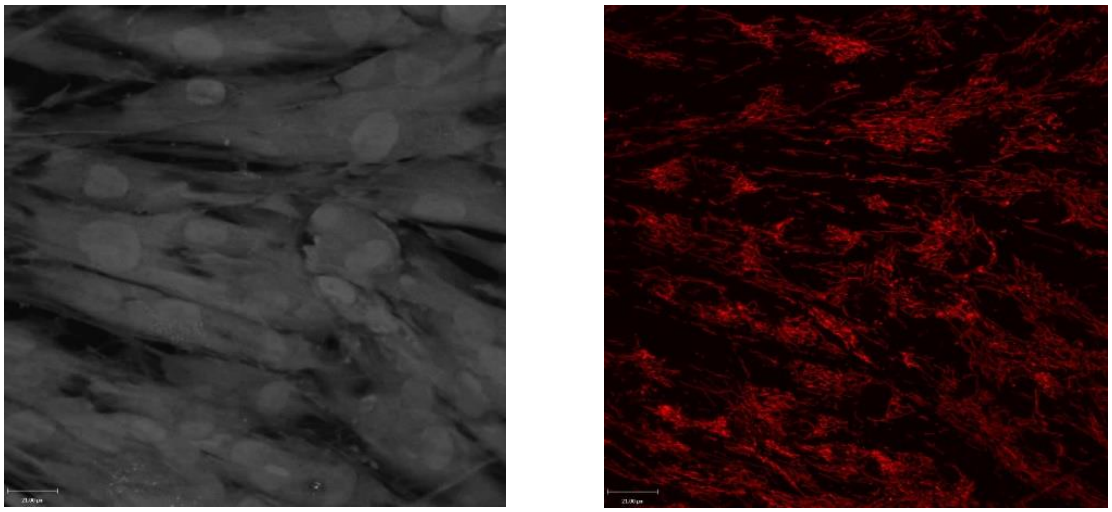

**(a)** **(b)**

**Figure 2.** Fibroblasts loaded with **(a)** Fura-2 AM for $Ca^{2+}$; **(b)** TMRM for mitochondrial membrane potential measurements. n=60.

The crown ethers 4',4"(5")-dibutyryl-DB18C6 and 4',4"(5")-divaleryl-DB18C6 have been observed to increase intracellular calcium levels in fibroblasts, as indicated by enhanced calcium fluorescence. In contrast, 4',4"-diacetyl-DB18C6 does not induce any significant change in intracellular calcium fluorescence (Figure 3). Investigations into the effects of 4',4"-diacetyl-DB18C6, 4',4"(5")-dibutyryl-DB18C6, and 4',4"(5")-divaleryl-DB18C6 on mitochondrial membrane potential in fibroblasts have shown that these crown ethers do not cause significant changes. The mitochondrial membrane potential remained stable and within normal ranges upon exposure to each of these crown ethers, indicating that they do not substantially disrupt mitochondrial function (Figure 3).

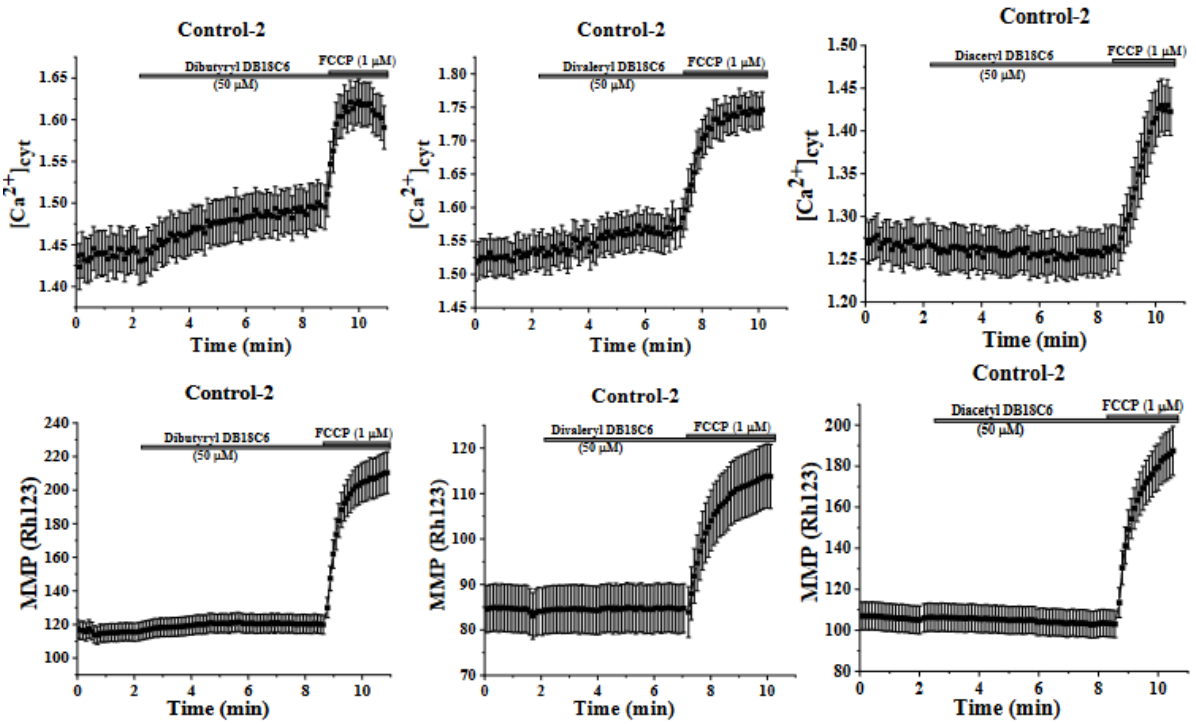


**Figure 3.** Fibroblasts loaded with Fura-2 AM for intracellular $Ca^{2+}$ and with TMRM for mitochondrial membrane potential determination, n=60.

*3.2. Diacyl derivatives of DB18C6 do not change intracellular pH in fibroblasts.*

Studied cell lines had no significant changes in intracellular pH in response to 50 µM of 4′,4″(5″)-dibutyryl-DB18C6 and 4′,4″(5″)-divaleryl-DB18C6 (Figure 4 A-B). Thus, the application of diacyl derivatives of DB18C6 does not induce cytosolic acidification in control fibroblasts.

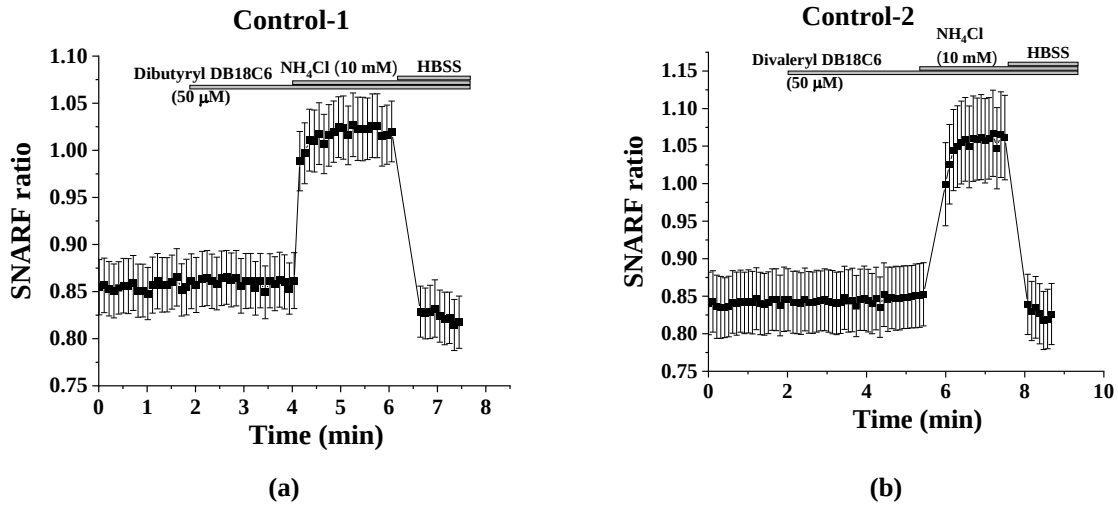


**Figure 4.** Control fibroblasts (a-b) loaded with SNARF AM for intracellular pH determination. n=60.

*3.3. Identification of the structure of diacyl derivatives of DB18C6.*

To determine the chemical structure of the reagents IR, $^{1}H$- and $^{13}C$-NMR spectra were obtained (Figure 5).

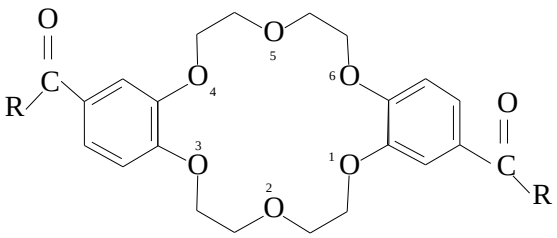


**Figure 5.** Chemical structure of diacyl derivatives of DB18C6.

Compounds characterized by little substituent position or length variation often show high spectral similarity (Figures 6-7). Computer-generated spectra and comparative analysis of these with experimental spectra are commonly employed in identifying molecular structures for new substances or sets of compounds [15-18].

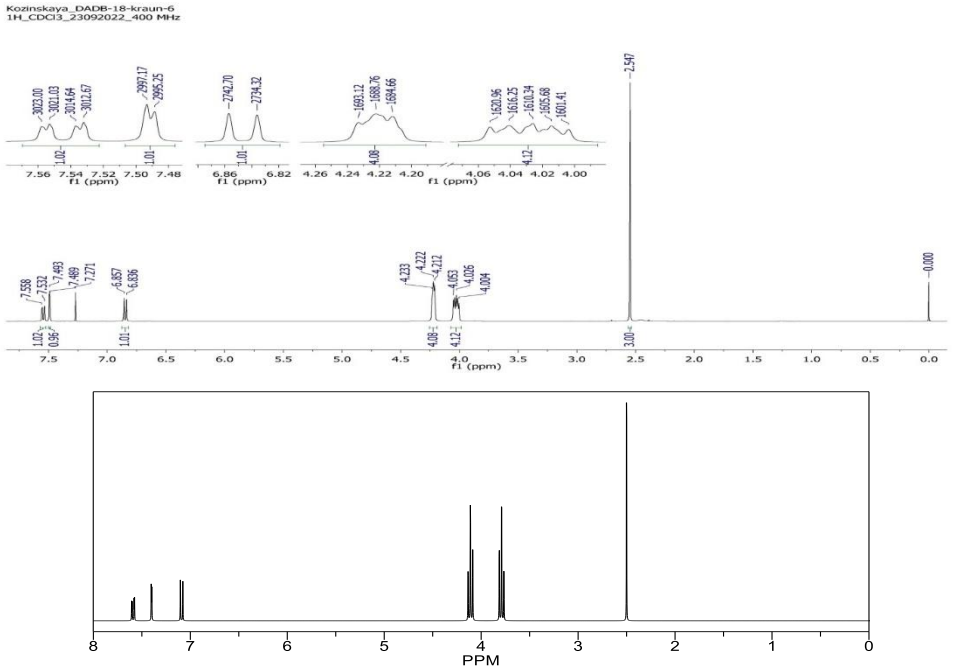


**(a)**

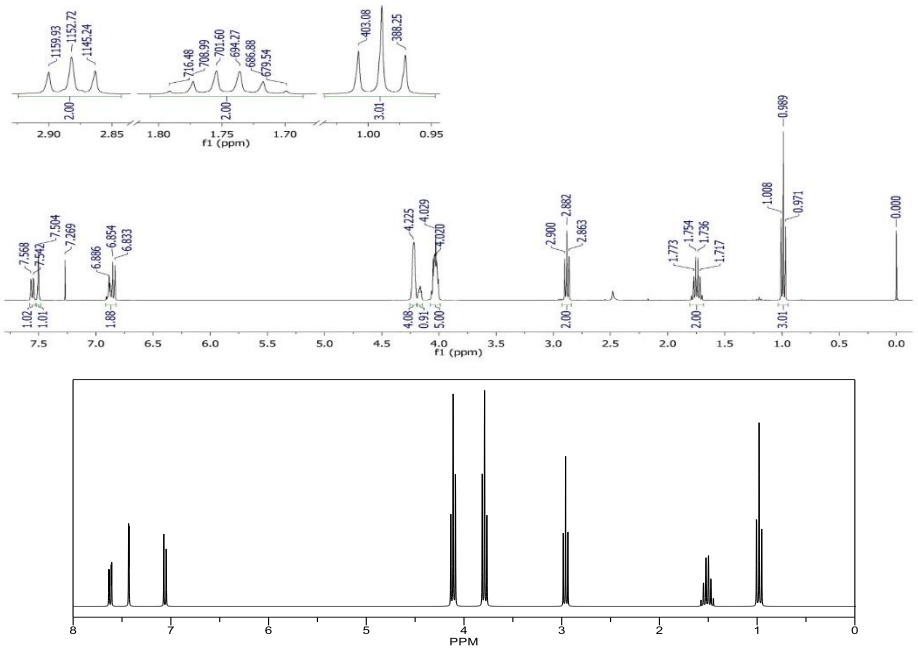


**(b)**

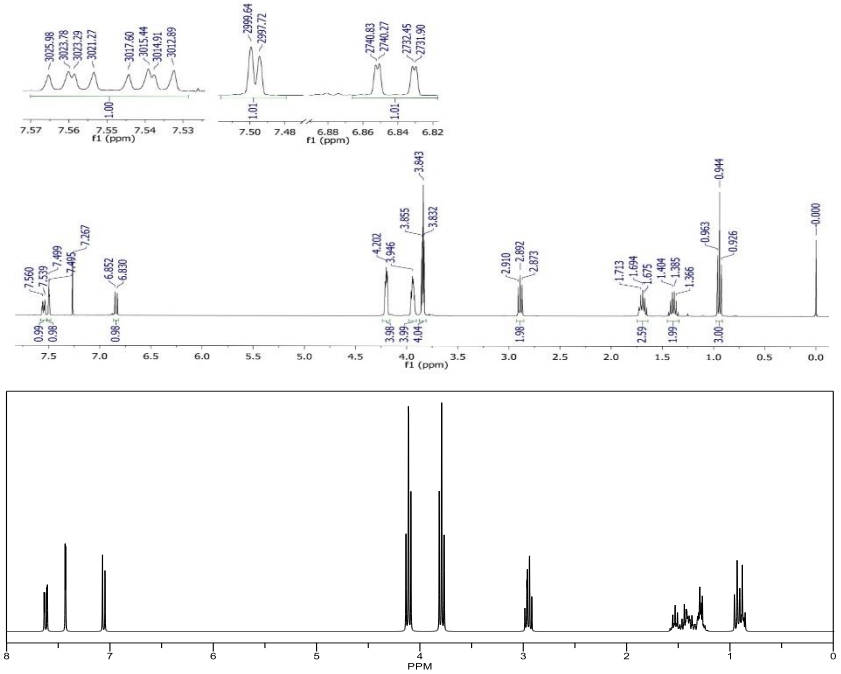

**(c)**

**Figure 6.** Calculation of $^{1}$H-NMR spectra of **(a)** 4',4''-diacetyl-DB18C6; **(b)** 4′,4″(5″)-dibutyryl-DB18C6; **(c)** 4′,4″(5″)-divaleryl-DB18C6.

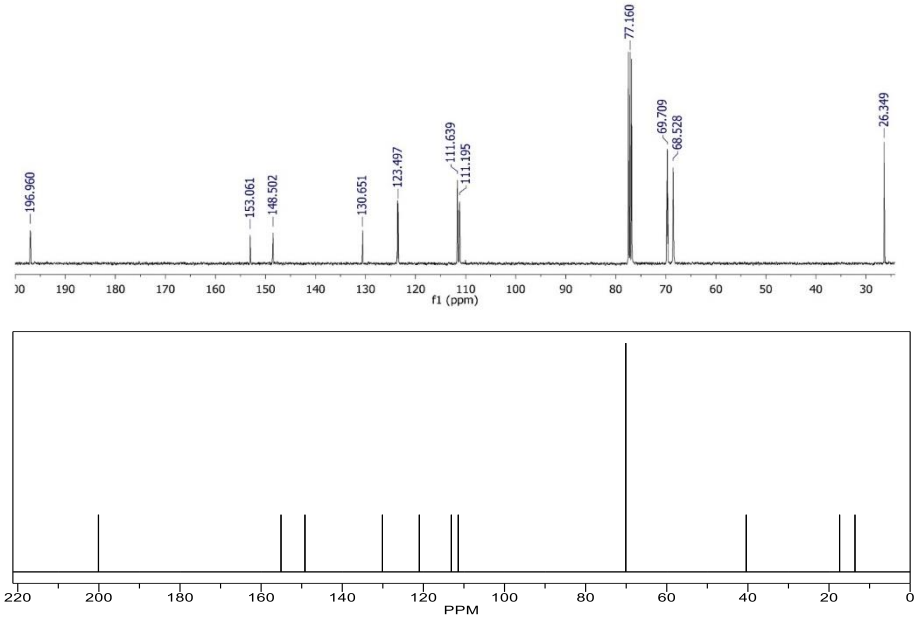

**(a)**

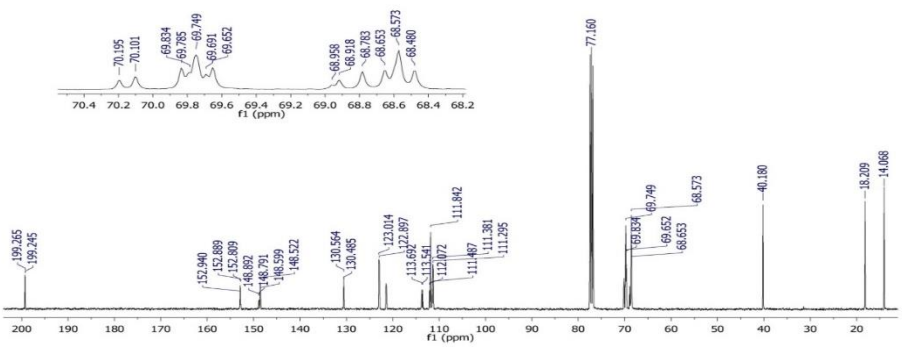

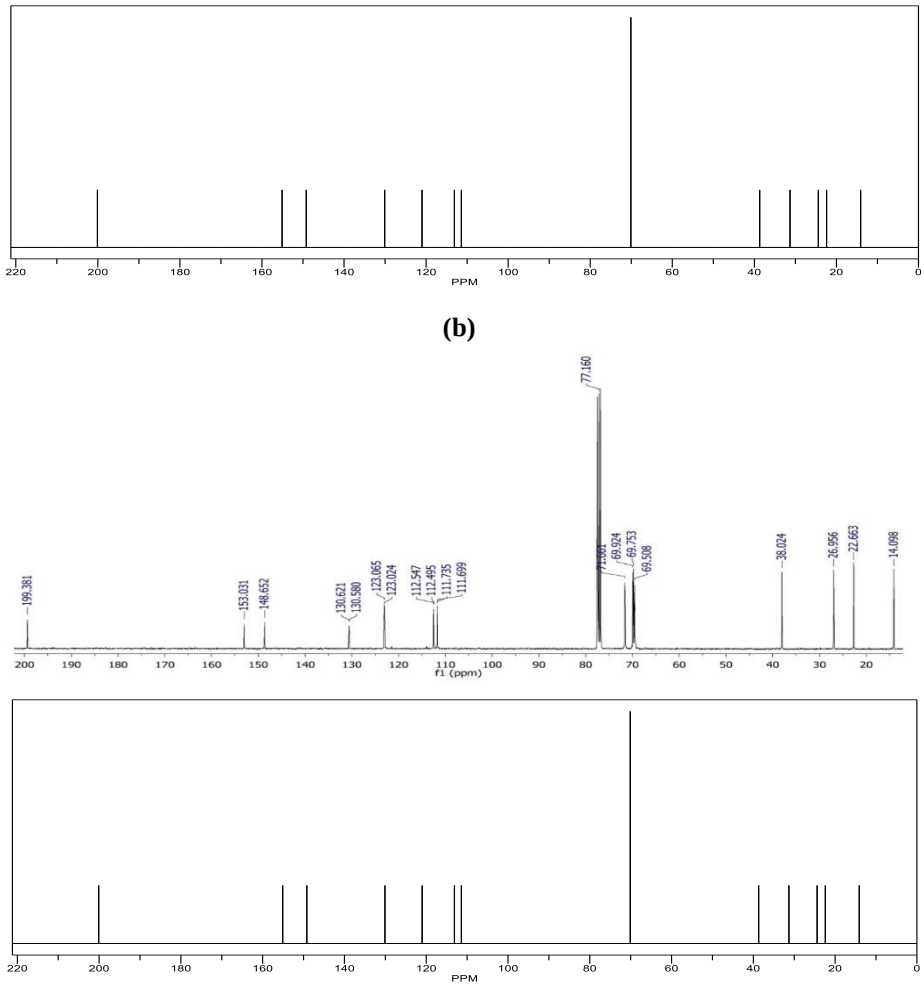


**Figure 7.** ChemNMR $^{13}C$ estimation for **(a)** 4′,4″(5″)-dibutyryl-DB18C6; **(b)** 4′,4″(5″)-divaleryl-DB18C6; **c)** 4′,4″(5″)-divaleryl-DB18C6.

Under the influence of substituents, the proton signals of the macrocycle (O-CH2) experience a shift towards a weaker region and appear at 4.00-4.23 ppm (Table 1). The calculated and recorded nuclear magnetic resonance (NMR) spectra exhibit an identical structure. This observation indicates the presence of all necessary functional groups and confirms the identification of the molecular structure.

**Table 1.** Comparison of experimental and calculated $^{1}H$-NMR spectra of 4',4"-diacetyl-DB18C6.

| | **α-$CH_3$** | **β-O-$CH_2$ α-O-$CH_2$** | **Ar-CH 6′,6″** | **Ar-CH 3′,3″** | **Ar-CH 5′,5″** |
|---|---|---|---|---|---|
| **Experimental data** | 2.54 | 4.00-4.05<br>4.21-4.23 | 6.83-6.85 | 7.48-7.49 | 7.53-7.55 |
| **Calculated spectra for 4',4"-diacetyl-DB18C6** | 2.50 | 3.79-4.11 | 7.09 | 7.40 | 7.59 |

The comparative analysis of the calculated and experimentally obtained $^{13}C$-NMR spectra of 4',4"(5")-diacetyl-DB18C6, 4′,4″(5″)-dibutyryl-DB18C6 and 4′,4″(5″)-divaleryl-DB18C6 indicates a congruence between the calculated predictions and the experimental findings (Table 2).

**Table 2.** Comparison of experimental and calculated $^{13}$C-NMR spectra of 4´,4´´-diacetyl- DB18C6.

| | **-CH₃** | **—C—** | **β-O-CH₂**<br>**α-O-CH₂** | **Ar-CH**<br>**3´,3´´**<br>**6´,6´´** | **Ar-CH**<br>**5´,5´´**<br>**4´,4´´** | **Ar-CH**<br>**1´,1´´**<br>**2´,2´´** |
|---|---|---|---|---|---|---|
| **Experimental data** | 26.34 | 196.96 | 68.52-69.70<br>77.16 | 111.19<br>111.63 | 130.65<br>123.49 | 153.06<br>148.50 |
| **Calculated spectra for 4',4"-diacetyl-DB18C6** | 26.6 | 197.0 | 70.1 | 110.0<br>111.4 | 128.9<br>121.0 | 155.1<br>149.2 |

Slight variations observed in the proton signals of $^{1}$H-NMR, as well as in the hydrocarbons of the aromatic ring in $^{13}$C-NMR spectra, and changes detected in the absorption bands of the infrared (IR) spectrum may be attributed to factors such as the spatial arrangement of the molecule, solvent interactions, or mutual influence of atomic groups (Table 1 and 2, Figure 7).

Crown ethers possessing ionophoretic properties demonstrate a dose-dependent increase in $Ca^{2+}$ transport across fibroblast membranes. The management of mitochondrial quality encompasses multiple pathways that regulate the degradation of mitochondria or mitophagy, thereby sustaining their functional activity throughout the cell's lifetime [19]. Currently, various mechanisms are known to stimulate mitophagy [20], one of which is the $Ca^{2+}$ concentration. Significant knowledge gaps exist regarding the contributions of $Ca^{2+}$ to the neuronal degeneration observed in Parkinson's disease. One such gap pertains to the interactions between genetic mutations associated with Parkinson's disease and $Ca^{2+}$-activated processes within substantia nigra pars compacta dopamine neurons. While dopamine may play a central role, $Ca^{2+}$ is the primary candidate for rendering these mutations detrimental. Addressing these knowledge gaps has potential implications for developing novel treatment approaches to prevent or mitigate the onset of Parkinson's disease and promote successful aging more broadly [21].

## 4. Conclusion

In this study, we investigated the efficacy of 4′,4″(5″)-dibutyryl-DB18C6 and 4′,4″(5″)-divaleryl-DB18C6 as alternative ionophores to specific ionophores. They were evaluated for their ability to act as ionophores for $Ca^{2+}$ ions at 10 and 100 nM concentrations. The investigated compounds demonstrated a dose-dependent induction of $Ca^{+2}$ permeability in the membranes of control fibroblasts, leading to an increase in intracellular $Ca^{+2}$ concentration.

Upon the completion of 30 years, it was determined that no chemical alterations had occurred within the reagents 4',4"-diacetyl-DB18C6, 4′,4″(5″)-dibutyryl-DB18C6 and 4′,4″(5″)-divaleryl-DB18C6.

## Funding

This work was supported by the Foundation for Development and Material Incentives of the Faculty and Students of the National University of the Republic of Uzbekistan, named after Mirzo Ulugbek.

## Acknowledgments

Our thanks go to Mrs. Aynisa.K.Tashmukhamedova and her team, who synthesized and kindly provided our experiments with suitable crown ethers for making all the above-discussed measurements [22,23].

## Conflict of interest

The authors declare no conflict of interest. The funding sponsors had no role in the design of the study, in the analyses, in the writing of the manuscript, and in the decision to publish the results.

## References


1. Bisi, N.; Feni, L.; Peqini, K.; Pérez-Peña, H.; Ongeri, S.; Pieraccini, S.; Pellegrino, S. α-Synuclein: An All-Inclusive Trip Around its Structure, Influencing Factors and Applied Techniques. *Front. Chem.* **2021**, *9*, 666585, https://doi.org/10.3389/fchem.2021.666585.
2. Ramezani, M.; Wagenknecht-Wiesner, A.; Wang, T.; Holowka, D.A.; Eliezer, D.; Baird, B.A. Alpha synuclein modulates mitochondrial $Ca^{2+}$ uptake from ER during cell stimulation and under stress conditions. *NPJ Parkinson's Dis.* **2023**, *9*, 137, https://doi.org/10.1038/s41531-023-00578-x.
3. Erustes, A.G.; Guarache, G.C.; Guedes, E.d.C.; Leão, A.H.F.F.; Pereira, G.J.d.S.; Smaili, S.S. α-Synuclein Interactions in Mitochondria-ER Contacts: A Possible Role in Parkinson's Disease. *Contact* **2022**, *5*, 25152564221119347, https://doi.org/10.1177/25152564221119347.
4. Paillusson, S.; Gomez-Suaga, P.; Stoica, R.; Little, D.; Gissen, P.; Devine, M.J.; Noble, W.; Hanger, D.P.; Miller, C.C.J. α-Synuclein binds to the ER–mitochondria tethering protein VAPB to disrupt $Ca^{2+}$ homeostasis and mitochondrial ATP production. *Acta Neuropathol.* **2017**, *134*, 129-149, https://doi.org/10.1007/s00401-017-1704-z.
5. Hotka, M.; Cagalinec, M.; Hilber, K.; Hool, L.; Boehm, S.; Kubista, H. L-type $Ca^{2+}$ channel-mediated $Ca^{2+}$ influx adjusts neuronal mitochondrial function to physiological and pathophysiological conditions. *Sci. Signal.* **2020**, *13*, eaaw6923, https://doi.org/10.1126/scisignal.aaw6923.
6. Arnst, N.; Redolfi, N.; Lia, A.; Bedetta, M.; Greotti, E.; Pizzo, P. Mitochondrial $Ca^{2+}$ Signaling and Bioenergetics in Alzheimer's Disease. *Biomedicines* **2022**, *10*, 3025, https://doi.org/10.3390/biomedicines10123025.
7. Yu, Z.; Wang, H.; Tang, W.; Wang, S.; Tian, X.; Zhu, Y.; He, H. Mitochondrial $Ca^{2+}$ oscillation induces mitophagy initiation through the PINK1-Parkin pathway. *Cell Death Dis.* **2021**, *12*, 632, https://doi.org/10.1038/s41419-021-03913-3.
8. Jadiya, P.; Cohen, H.M.; Kolmetzky, D.W.; Kadam, A.A.; Tomar, D.; Elrod, J.W. Neuronal loss of NCLX-dependent mitochondrial calcium efflux mediates age-associated cognitive decline. *iScience* **2023**, *26*, 106296, https://doi.org/10.1016/j.isci.2023.106296.
9. Verma, M.; Lizama, B.N.; Chu, C.T. Excitotoxicity, calcium and mitochondria: a triad in synaptic neurodegeneration. *Transl. Neurodegener.* **2022**, *11*, 3, https://doi.org/10.1186/s40035-021-00278-7.
10. Kim, S.; Kim, D.K.; Jeong, S.; Lee, J. The Common Cellular Events in the Neurodegenerative Diseases and the Associated Role of Endoplasmic Reticulum Stress. *Int. J. Mol. Sci.* **2022**, *23*, 5894, https://doi.org/10.3390/ijms23115894.
11. Virdi, G.S.; Choi, M.L.; Evans, J.R.; Yao, Z.; Athauda, D.; Strohbuecker, S.; Nirujogi, R.S.; Wernick, A.I.; Pelegrina-Hidalgo, N.; Leighton, C.; Saleeb, R.S.; Kopach, O.; Alrashidi, H.; Melandri, D.; Perez-Lloret, J.; Angelova, P.R.; Sylantyev, S.; Eaton, S.; Heales, S.; Rusakov, D.A.; Alessi, D.R.; Kunath, T.; Horrocks, M.H.; Abramov, A.Y.; Patani, R.; Gandhi, S. Protein aggregation and calcium dysregulation are hallmarks of familial Parkinson's disease in midbrain dopaminergic neurons. *NPJ Parkinson's Dis.* **2022**, *8*, 162, https://doi.org/10.1038/s41531-022-00423-7.
12. Xu, J.; Minobe, E.; Kameyama, M. $Ca^{2+}$ Dyshomeostasis Links Risk Factors to Neurodegeneration in Parkinson's Disease. *Front. Cell. Neurosci.* **2022**, *16*, 867385, https://doi.org/10.3389/fncel.2022.867385.
13. Uspalenko, N.I.; Mosentsov, A.A.; Khmil, N.V.; Pavlik, L.L.; Belosludtseva, N.V.; Khunderyakova, N.V.; Shigaeva, M.I.; Medvedeva, V.P.; Malkov, A.E.; Kitchigina, V.F.; Mironova, G.D. Uridine as a Regulator of Functional and Ultrastructural Changes in the Brain of Rats in a Model of 6-OHDA-Induced Parkinson's Disease. *Int. J. Mol. Sci.* **2023**, *24*, 14304, https://doi.org/10.3390/ijms241814304.
14. Iqbal, T.; Arshad, N.; Hashim, J.; Ali, S.A.; Zehra, B.; Ahmad, M.S.; Hassan, N.; Ullah, A.; Hamid, S.Z.; Isaac, I.O. Natural products based crown ethers: synthesis and their anticancer potential. *J. Asian Nat. Prod. Res.* **2022**, *24*, 268-277, https://doi.org/10.1080/10286020.2021.1918118.

15. Arkhipov, V.P.; Arkhipov, R.V.; Kuzina, N.A.; Filippov, A. Study of the premicellar state in aqueous solutions of sodium dodecyl sulfate by nuclear magnetic resonance diffusion. *Magn. Reson. Chem.* **2021**, *59*, 1126-1133, https://doi.org/10.1002/mrc.5165.
16. Qi, Z.; Qin, Y.; Wang, J.; Zhao, M.; Yu, Z.; Xu, Q.; Nie, H.; Yan, Q.; Ge, Y. The aqueous supramolecular chemistry of crown ethers. *Front. Chem.* **2023**, *11*, 1119240, https://doi.org/10.3389/fchem.2023.1119240.
17. Ullah, F.; Khan, T.A.; Iltaf, J.; Anwar, S.; Khan, M.F.; Khan, M.R.; Ullah, S.; Fayyaz ur Rehman, M.; Mustaqeem, M.; Kotwica-Mojzych, K.; Mojzych, M. Heterocyclic Crown Ethers with Potential Biological and Pharmacological Properties: From Synthesis to Applications. *Appl. Sci.* **2022**, *12*, 1102, https://doi.org/10.3390/app12031102.
18. Duan, Z.; Xu, F.; Huang, X.; Qian, Y.; Li, H.; Tian, W. Crown Ether-Based Supramolecular Polymers: From Synthesis to Self-Assembly. *Macromol. Rapid Commun.* **2022**, *43*, 2100775, https://doi.org/10.1002/marc.202100775.
19. Kaur, S.; Sehrawat, A.; Mastana, S.S.; Kandimalla, R.; Sharma, P.K.; Bhatti, G.K.; Bhatti, J.S. Targeting calcium homeostasis and impaired inter-organelle crosstalk as a potential therapeutic approach in Parkinson's disease. *Life Sci.* **2023**, *330*, 121995, https://doi.org/10.1016/j.lfs.2023.121995.
20. Fedotova, E.I.; Dolgacheva, L.P.; Abramov, A.Y.; Berezhnov, A.V. Lactate and Pyruvate Activate Autophagy and Mitophagy that Protect Cells in Toxic Model of Parkinson's Disease. *Mol. Neurobiol.* **2022**, *59*, 177-190, https://doi.org/10.1007/s12035-021-02583-8.
21. Oguz, M.; Kalay, E.; Akocak, S.; Nocentini, A.; Lolak, N.; Boga, M.; Yilmaz, M.; Supuran, C.T. Synthesis of calix[4]azacrown substituted sulphonamides with antioxidant, acetylcholinesterase, butyrylcholinesterase, tyrosinase and carbonic anhydrase inhibitory action. *J. Enzyme Inhib. Med. Chem.* **2020**, *35*, 1215-1223, https://doi.org/10.1080/14756366.2020.1765166.
22. Tashmukhamedova A.K. **et. al.** Diacylates derivatives of 2,3,11,12-dibenzo-1,4,7,10,13,16-hexaoxacyclooctadeca-2,11-dien as regulator of ion permeability of biological membranes. Google Patents. SU644789A1. USSR. 1976.
23. Mirkhodzhaev, U.Z.; Boldyrev, V.A.; Tashmukhamedova, A.K.; Tatarskiĭ, V.P.; Dimant, I.N. Ion conductance channels of bilayer from sarcoma-45 phospholipids. *Biofizika* **1989**, *34*, 235-240.